Korean J. Chem. Eng., 36(10), 1565-1574 (2019)
DOI: 10.1007/s11814-019-0370-3

pISSN: 0256-1115
eISSN: 1975-7220

INVITED REVIEW PAPER

Electrospun nanofiber filters for highly efficient $PM_{2.5}$ capture

Changwoo Nam, Sukyoung Lee, Min Ryu, Jaewook Lee, and Hyomin Lee†

Department of Chemical Engineering, Pohang University of Science and Technology, (POSTECH),
77 Cheongam-ro, Nam-gu, Pohang, Gyeongbuk 37673, Korea
(*Received 15 June 2019 • accepted 19 August 2019*)

Abstract−With the recent increase of concern on the health impact of air pollution, there has been growing interest in filtration technologies that can effectively remove fine inhalable particles ($PM_{2.5}$) in the air with diameters that are generally 2.5 μm or smaller. Among various technologies presented, nanofiber-based filters provide A simple, but effective route to rapidly capture these fine particulate matters. In this review, we briefly introduce the health hazards associated with $PM_{2.5}$ and highlight the importance of air filtration technology with particular emphasis on nanofiber-based filters prepared *via* electrospinning. Then, we summarize various fiber materials and additives utilized in electrospun nanofibers to enhance the filtration efficacy. Furthermore, we highlight some of the recent advances in the materials design of electrospun nanofiber filters for $PM_{2.5}$ removal and discuss the current issues and future perspectives.

Keywords: Particulate Matter ($PM_{2.5}$), Electrospinning, Filter, Polymeric Materials, Nanofiber

INTRODUCTION

Concerns regarding air pollution and health hazards from fine dust particles in the atmosphere are being steadily raised [1]. In particular, Korea has been under siege by the worst haze problem over the past few years caused by the fine particle pollutants in the atmosphere, possibly due to the increase in the number of coal-based power plants and diesel fuel operated vehicles in Korea, as well as the sharp increase in fossil fuel usage in nearby developing countries such as China, leading to public awareness about the fine particles in the air and their impact on health [2,3].

Particulate matter (PM), by definition, is the sum of all solid particles, liquid droplets suspended in the air. Based on size, PM can be divided into PM_{10} and $PM_{2.5}$, in which the subscript denotes the upper bound of the particulate diameter in micrometers [4]. The particle diameter determines the aerodynamic properties and thus governs how far they can get into the air passages of an individual's respiratory system. In fact, small particles can penetrate the pulmonary alveoli and enter into the circulatory system, inducing severe health problems [5,6]. Numerous studies have linked these ultrafine particle exposures to a variety of symptoms, especially to respiratory and cardiovascular diseases [7,8].

To reduce the risk of exposure and provide protection against these ultra-fine particles ($PM_{2.5}$), various air cleaners based on cyclones, electrostatic precipitation, and scrubbers have been employed [9]. While these methods allow easy removal of larger particles, they are ineffective for small particles (<10 μm). For instance, electrostatic precipitation is highly efficient in PM_{10} removal, but the dust removal effectiveness significantly diminishes as the particles size becomes smaller due to their low electrostatic charge efficiency. While high voltage pulse generators [10] have been exploited to provide additional charge for these smaller particles and achieve higher particle collection efficiency, they may produce ozone that can trigger the formation of secondary particles by reacting with the organic gases in the atmosphere [11,12].

Alternatively, filtration techniques by high efficiency particulate air (HEPA) filters with PM removal efficiency of about 99.97% for 0.3 μm airborne particles are widely applied for capturing ultra-fine particles [13]. HEPA filters exhibit high filtration efficiency and high-performance stability in various applications. However, the thick media required to achieve high filtration efficiency in these filters comprised of micro-scale fibers and pores often lead to either high pressure drop or energy cost to compensate the resulting flow resistance [14,15]. These drawbacks of conventional high performance filters can be alleviated by preparing nanofiber-based filters through electrospinning [16-21]. Electrospinning allows production of nano-scale fibers with diameters in the range of 40 to 2,000 nm. Moreover, the filters prepared from electrospun nanofibers have properties such as high surface-to-volume ratio, low pressure drop, and controllable morphology and connectivity, making them attractive for achieving excellent filtering performance of $PM_{2.5}$ at low cost [22,23].

In this review, we first introduce the mechanism of dust removal by these fibrous filters and briefly discuss the principles of electrospinning in preparing nanofiber filters. Then, we review the characteristics of various types of electrospun nanofiber filters, focusing on the recent advances in the materials design of electrospun nanofiber filters. Finally, conclusions will be briefly presented followed by the current challenges and future perspectives.

FILTRATION MECHANISMS

The performance of a filter to intercept particles in the air depends on the characteristics of the filter as well as particle size, surface charge, and the air flow velocity [24,25]. Thus, prior to discussing the electrospun fibers, we will briefly review classical filtration

†To whom correspondence should be addressed.
E-mail: hyomin@postech.ac.kr
Copyright by The Korean Institute of Chemical Engineers.

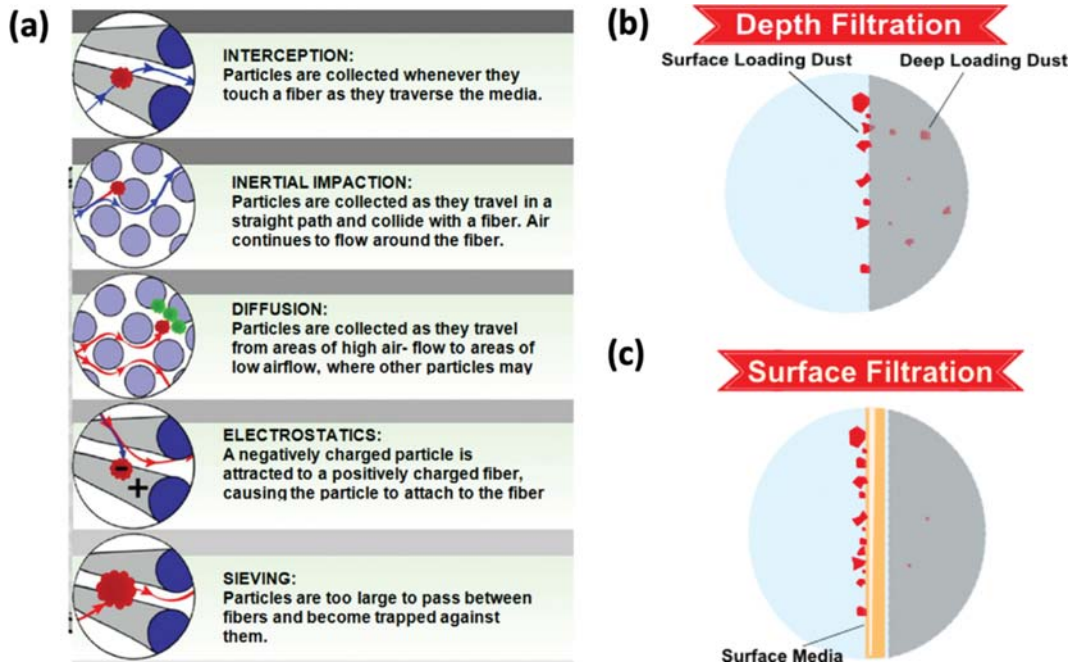

Fig. 1. (a) Schematics showing the five representative filtration mechanisms. (b)-(c) The comparison between (b) depth filtration and (c) surface filtration of PMs (modified from www.adebiotech.org).

theory which has been elaborated in detail by others [26,27].

Based on the classical filtration theory, fiber-based particle filtration can be categorized into five mechanisms: sieving, interception, inertial impaction, diffusion, and electrostatic interaction (Fig. 1(a)). In sieving, particles larger than the gap between the fibers can be trapped by the size mismatch. Conventional microfiber-based filters often rely on this size-mismatch to remove large particulate matter (>$PM_{2.5}$) in the air. On the other hand, when finer particles travel along with the air and approach the surface of the irregularly aligned fibers at low flow rates, the fibers can intercept the aerosol particle upon contact due to van der Waals interaction. At high air flow rates, however, particles initially intercepted on the surface can be detached. This interception is the most important PM removal mechanism for PM in the range of 0.1-1 μm and the removal efficiency scales with increase in particle size [28]. For larger particles (>1 μm) operated at high air flow velocities, the densely packed nature of the fiber within the filter often causes these large particles to deviate from the air flow line and attach to the fibers due to inertial impaction [29]. However, for $PM_{0.1}$ smaller than 0.1 μm in diameter, the particles exhibit significant random Brownian motion, resulting in diffusion and deposition of particles [30]. In electrostatic interaction, charged aerosol particles can adhere to oppositely charged fiber surface due to columbic interaction and polarization forces. The additional contribution of electrostatic interaction allows particles to more firmly attach to the fiber surface and enhance the removal efficiency without increase of pressure drop. Hence, electrostatic interaction is often utilized to capture particles with size near 0.3 μm or smaller which cannot be effectively removed even with nanofiber filters.

Different filtration mechanisms dominate for varying particle size, air flow rate, as well as the presence of surface charge. Among these mechanisms, sieving is the simplest approach to remove PMs by using a filter with spacing between the fibers that are smaller than the PM size [31]. However, as the sieving continues, the PM removal efficiency and flow resistance change over time due to PMs collected in the spacing of the fiber network. While subsequent PMs can be more easily captured in these particles accumulated fiber network by a phenomenon known as depth filtration [32] in conventional micro-scale fibers, long-term usage leads to high pressure drop and decrease in filtration efficiency (Fig. 1(b)). Moreover, particle deposition throughout the fiber network in depth loading makes it difficult to rinse off the PMs in the clogged filter network without damaging the filter, limiting the reuse of filters.

Unlike these conventional filters, filters comprised of nano-scale fibers allow the collection of $PM_{2.5}$ on the filter surface [33]. Due to the surface filtration of particles in these nanofiber filters [34], the pressure drop is less compared to conventional filters during filtration process and offer energy saving by reducing the energy required to offset the pressure drop (Fig. 1(c)). Furthermore, the $PM_{2.5}$ collected can be easily removed as most of the particles are positioned on the filter surface instead of the whole filter network. The ability to effectively remove $PM_{2.5}$ in the air and retain high PM removal efficiency and low pressure drop even after long-term usage is one of the hallmarks of nanofiber-based filters [35,36].

ELECTROSPINNING TECHNOLOGY

To prepare these nanofiber-based filters with excellent properties, various techniques such as bi-component spinning, melt-blowing spinning, flash spinning, and electrospinning methods have been explored. Among these, electrospinning is one of most effective techniques to fabricate nanofibers, as it offers a simple process, inex-

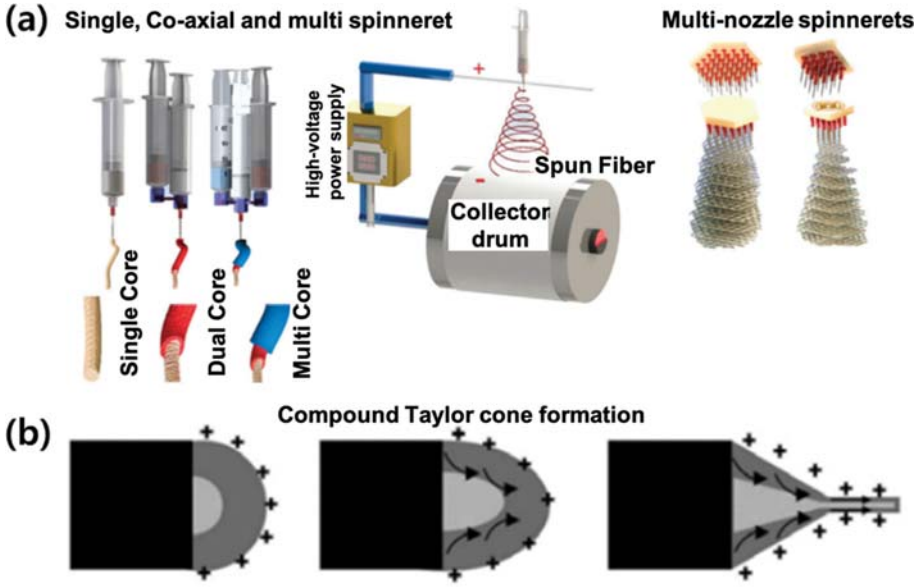

Fig. 2. Schematic illustration of (a) the experimental setup used for preparing electrospun nanofibers with various structures [38] and (b) the compound Taylor cone formation: (Left) Surface charges on the sheath polymer solution, (middle) Viscous drag exertion on the core, (right) Sheath-core compound Taylor cone formation [39].

pensive cost, as well as precise control over the compositions and geometrical characteristics of the nanofibers [37].

In electrospinning, four major components are required to fabricate nanofibers: a syringe pump, a high voltage power supply, a spinneret, and a collector (Fig. 2(a)) [38]. With the use of a syringe pump, polymer solution can be injected at a precisely controlled rate. The high voltage power supply allows charging of the solution by connecting to the tip of the syringe needle called spinneret as well as the metallic collector that is grounded.

When the applied voltage exceeds the critical value to overcome the surface tension of the solution, the charged fluid droplet forms a Taylor cone (Fig. 2(b)). Then, from the head of the Taylor cone, the ejected solution elongates in the form of a jet with the electric field. This is followed by evaporation of the solvent and deposition of nanoscale polymeric fibers onto the metal collector, resulting in a non-woven fabric [39].

To acquire nanofibers with the desired composition, morphology, and size through electrospinning, various electrospinning parameters need to be considered [40]. In the materials design perspective, the solution properties such as conductivity, surface tension, volatility, and viscosity are most crucial in the electrospinning process. When selecting a solvent to dissolve the polymeric material of interest for electrospinning, a solvent with high conductivity is necessary and often may require additional salts or mixing with other conductive solvents [41]. Increasing the conductivity of the solution grants good transmission of the electromagnetic field to the solvent, leading to strong electrostatic repulsion to overcome the surface tension and thus formation of fibers. Moreover, the dielectric constant (ε) of the solvent also affects the resulting fiber diameter. Higher dielectric constant of the solvent enhances the effect of electrostatic repulsion, enabling production of thinner fibers under constant operating conditions. By contrast, thicker and reduced number of jets are ejected even at high voltage for solvents with low dielectric constant (ε<10) [42].

Regardless of conductivity, when the volatility of the solution is too low, the solvent in the ejected jet has insufficient time to evaporate before depositing onto the collector, forming a wet fiber. On the other hand, if the solution is too volatile, evaporation may occur too quickly and become fibrous from the tip end, leading to unstable spinning.

Furthermore, the interaction between the polymer chain of interest as well as the solvent may increase the viscosity of the solution. For such highly viscous solution, it is difficult to uniformly dissolve the polymer in the solution during preparation and to stretch the polymer solution in the form of jet to make nanofibers during electrospinning process. In such case, extremely high electrical charge is needed to eject the solution from the tip of the spinneret.

Based on the effect of electrospinning process parameters described so far, it may seem that polar solvent such as water with high surface tension and low volatility cannot be used for preparing nanofibers. Indeed, the aqueous solution typically does not completely evaporate prior to reaching the collector. Thus, the ejected solution often falls in the form of droplets instead of a continuous jet. However, by mixing with other solvents that can lower the surface tension of water, continuous jet can be formed to prepare nanofibers [43,44]. More detailed description of other polymer solutions investigated in electrospinning as well as processing and ambient parameters in preparing nanofibers such as flow rate, humidity, tip to collector distance, and temperature can be found in other reviews [45-47].

ELECTROSPUN NANOFIBER-BASED FILTERS

Electrospun nanofibers exhibit excellent properties, including high porosity, high surface-to-volume ratio, and uniform fiber size, fulfilling the key requirements of an excellent filter for capturing

ultra-fine dusts [48]. The performance of these filters is mainly determined by the structural properties of the electrospun nanofibers. In particular, the structure of the fibrous membrane such as fiber diameter, surface area, fiber basis weight and thickness has a significant effect on the filtration efficiency as well as the associated pressure drop [49,50]. In addition to these structural properties, the filtration performance is also largely dependent on the physical properties of the nanofiber filters as well as the particular filtering factors such as particle size, air flow velocity, temperature, and humidity [51]. In this section, we will focus on properties such as structural, mechanical, optical, and thermal that are all related to the functions of these newly developed electrospun nanofiber filters. We will also discuss the recent progress made in the design of electrospun nanofibers, summarizing various polymeric fiber materials and additives utilized to enhance the filtration performance.

STRUCTURAL PROPERTY OF NANOFIBER FILTERS

To date, a library of polymers has been exploited for electrospun nano-fibrous filters [52,53]. However, filters comprised of a unitary polymer usually do not fulfill all the properties required for achieving high filtration performance such as high filtration efficiency, low pressure drop, high mechanical durability, and additional functionalities required depending on the specific application.

To resolve this issue, many researchers have investigated composite air filters in which two components with complementary functions are incorporated in a filter membrane [54,55]. These dual component nanofiber filters exhibit more than two characteristics such as excellent $PM_{2.5}$ removal efficiency, mechanical durability, and multi-functionality within a single filter. While dual component nanofibers are conventionally prepared by blending two poly-

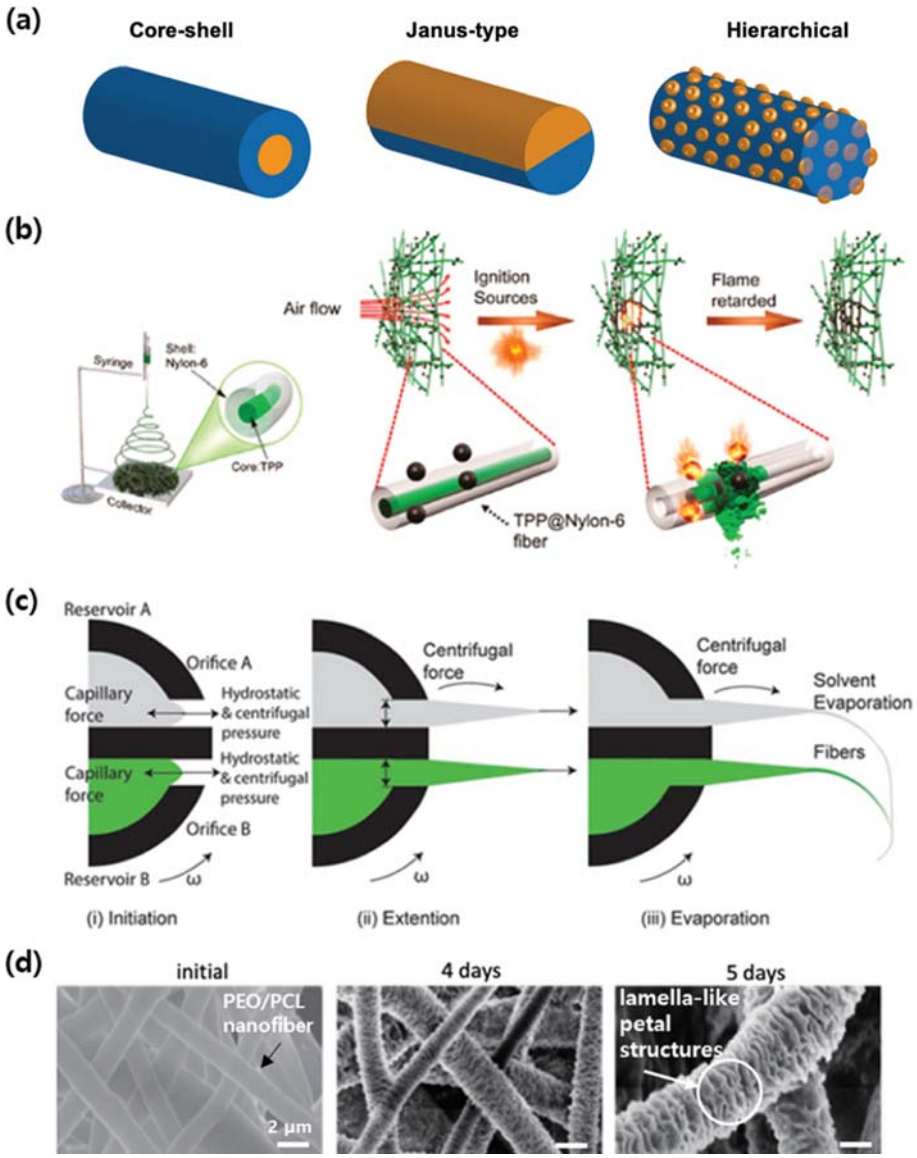

Fig. 3. (a) Schematic showing the bi-phasic fiber morphologies with core-shell (left), Janus type (middle) and hierarchical structures (right). (b) Fabrication of the core (TPP)-shell (Nylon-6) nanofibers by electrospinning [60]. (c) The centrifugal jet spinning process to produce Janus-type nanofibers [61]. (d) SEM images of the PCL/PEO nanofibers with various exposure times to acetone vapor [62].

mers [56], introducing guest materials [57], and multi-layering of nano-fibrous membranes [58], more advanced structural designs are being currently exploited which can be classified into core-shell, Janus-type and hierarchical structures (Fig. 3(a)). These designs allow fabrication of nanofiber membranes with high filtration performance as well as additional functionality without compromising the flow resistance [59].

For instance, Liu et al. developed a core-shell structured nanofiber filter which exhibits excellent $PM_{2.5}$ removal efficiency, low pressure drop, and flame retardant property [60]. This core-shell structure nanofiber filter comprises a flame retardant triphenyl phosphate (TPP) core and a Nylon-6 shell as shown in Fig. 3(b). Due to the presence of TPP serving as a radical scavenger, the $PM_{2.5}$ collected on the nanofiber filter can be eliminated by igniting without the filter snapping at high temperature. Additionally, this nanofiber filter exhibits high optical transparency (80%), high removal efficiency of $PM_{2.5}$ (99.00%) and PM_{10} (99.50%), and low pressure drop (0.25 kPa).

A Janus-type nanofiber allows access to two different materials while retaining a reasonably large contact area. Khang et al. demonstrated a bi-phasic Janus-type polymer nanofibers (BJPNF) with highly aligned biphasic materials by centrifugal jet spinning (CJS) with a dual-reservoir nozzle (Fig. 3(c)) [61]. The bi-phasic Janus-type nanofibers comprised of polycaprolactone (PCL) and gelatin were prepared by adjusting the polymer solution concentrations and the rotation speed during fabrication to obtain large enough capillary number for the formation of continuous fibers instead of particles. These BJPNFs are potentially useful for applications that require different properties on either side of the fiber.

Hierarchically structured nanofibers with additional nanoscale sub features provide larger surface area and thus enhanced ultrafine dust removal efficiency. Recently, Huang et al. prepared a nanocomposite air filtration matrix comprising of poly (ε-caprolactone)/polyethylene oxide (PCL/PEO) using an electrospinning technique and subsequent solvent vapor annealing (SVA) with acetone vapor. The SVA treatment induced formation of self-organized hierarchical nanostructures (lamella-like petal structure) as shown in Fig. 3(d), which enabled high $PM_{2.5}$ removal efficiency even under heavily polluted conditions [62].

PHYSICAL PROPERTY OF NANOFIBER FILTERS

We next highlight the physical property of the electrospun nanofiber filters, including mechanical, optical, and thermal, which all enable preparation of high-performance nano-fibrous membranes with desirable functionalities.

MECHANICAL PROPERTY OF NANOFIBER FILTERS

It is essential for the electrospun nanofiber filters to have sufficient mechanical strength to maintain the filter structure under constant air pressure. To increase the mechanical strength of the electrospun nanofibers, two different strategies have been explored: one is to utilize polymers with high mechanical strength such as polypropylene (PP) [63], and the other is to blend polymer of interest with guest materials such as cross-linkers, carbon nanotubes (CNT) or glass fibers.

Zhang et al. added poly (ethylene oxide) (PEO) to polyacrylonitrile/polysulfone (PAN/PSU) fiber composite membranes, which has high chemical stability and weatherability to fabricate filters with

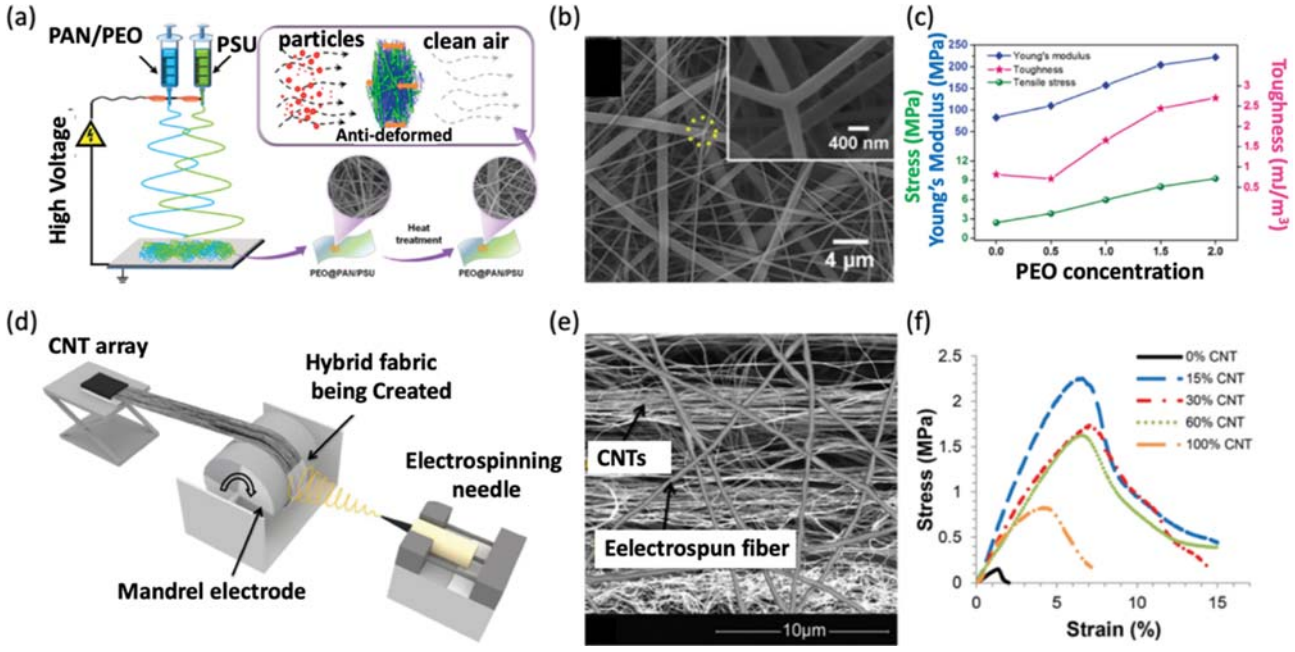

Fig. 4. (a) Schematics illustrating the fabrication of nanofiber filter based on PAN, PEO and PSU. (b) SEM image of PEO reinforced PAN/PSU fiber composite membranes. (c) Mechanical properties of the PEO reinforced PAN/PSU fiber composite membranes [64]. (d) Schematic of the nanofiber fabrication process with aligned CNT sheets and (e) SEM image of 30% CNT hybrid nanofiber. (f) Stress-strain curve of PAN/PEO nanofiber with different CNT ratios [65].

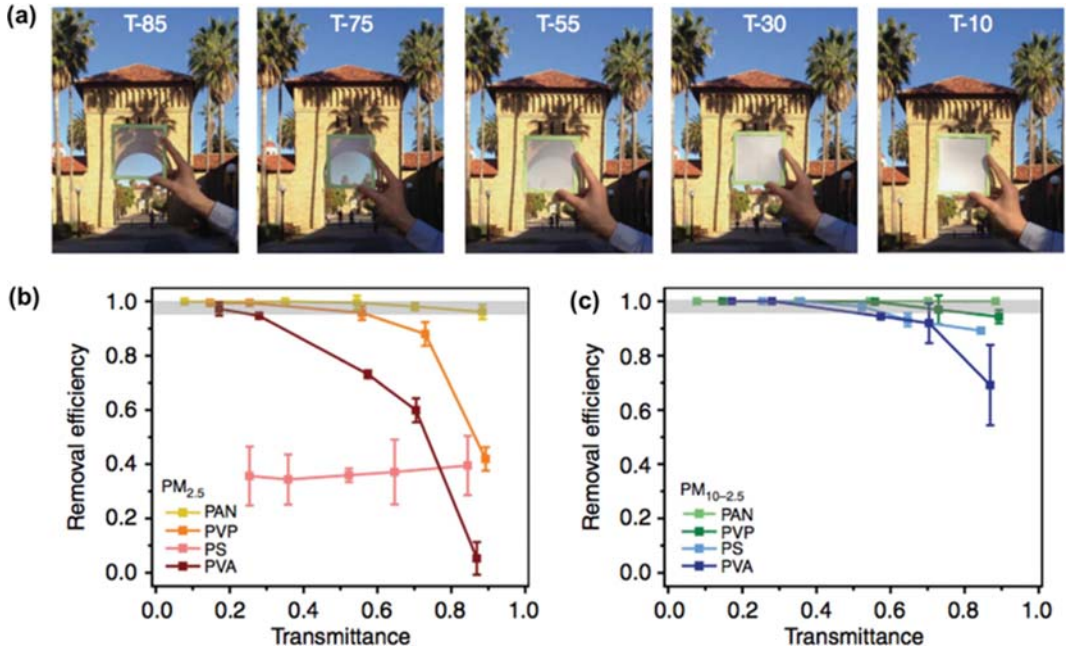

Fig. 5. (a) Photograph images of PAN filters with different level of optical transparency. (b) $PM_{2.5}$ removal and (c) $PM_{10\text{-}2.5}$ collection efficiencies of PAN, PVP, PS, and PVA filters at different level of transmittances [67].

excellent physical properties [64]. These nanofibers were fabricated using a multi-jet electrospinning method in which PAN nanofibers and PSU microfibers were uniformly aligned. The number of fibers gradually increased while the overall pressure drop was lowered when the mixing ratio of PSU to PAN increased. The addition of PEO to copolymer increased the mechanical strength of the PAN/PSU filter by providing interconnection between the fibers (Fig. 4(a)-(b)). They also confirmed that increasing the concentration of PEO (0-2.5 wt%, as a bonding agent) led to formation of physical bonding among the fibers, resulting in a dramatic increase in the mechanical strength. The optimized filters exhibited high tensile strength (8.2 MPa), stiffness (2.44 MJ/m^3), and low pressure drop (<8 Pa) (Fig. 4(c)) with high filtration efficiency (99.992%).

Yildiz et al. reported a series of hybrid filters in which PEO was mixed with CNT in different ratios (0, 15, 30, 60, and 100% CNT sheet) to prepare nanofiber filters that have excellent mechanical and chemical properties as well as ultra-fine dust removal efficiency similar to HEPA and ULPA filter (Fig. 4(d)-(e)) [65]. Note that the hybrid filter fabricated under high temperature (70 °C) and high pressure (2 MPa) condition exhibited uniform distribution of PEO and CNT over a wide area for up to 30% of CNT content (Fig. 4(f)). However, when the CNT content exceeded 30%, phase separation between CNT and PEO-based nanofiber occurred, which dramatically decreased the mechanical properties. This reveals that the uniformity of the nanofiber is important for achieving enhanced mechanical strength.

OPTICAL PROPERTY OF NANOFIBER FILTER

Filters with high $PM_{2.5}$ capture efficiency and good optical transparency offer a facile route to exchange outdoor air as well as sufficient transmission of light without the concern of additional intake of ultra-fine dust from outside.

Electrospinning allows fabrication of filters with nanofibers that have high $PM_{2.5}$ capture efficiency as well as outstanding optical properties compared to microfiber filters [66]. Liu et al. proposed the application of PAN based nanofiber filters with excellent transparency and high filtration efficiency on the windows of a building [67]. These PAN based nanofiber filters exhibited high $PM_{2.5}$ removal efficiency (96.12%), low pressure change. Additionally, the filters had excellent optical transparency (about 85%) compared to a conventional air filter (15%) as well as polystyrene (PS), polyvinyl alcohol (PVA), and polyvinylpyrrolidone (PVP) based nanofiber filters as shown in Fig. 5(a)-(c).

NANOFIBER FILTERS WITH HIGH THERMAL STABILITY

In general, electrospun nanofiber filters are designed to operate at room temperature and cannot endure elevated temperatures, limiting their application for capturing $PM_{2.5}$ in high temperature conditions such as coal plant and manufactory.

To filter ultra-fine dusts in a high temperature environment, filters that retain mechanical stability in high temperature are needed [33]. Wang et al. fabricated yttria-stabilized ZrO_2 (YSZ) filters that have high heat resistance and excellent $PM_{2.5}$ removal ability by using $Ti(OBu)_4$/PVP based solution and high temperature gas supply (Fig. 6(a)) [68]. Specifically, YSZ filters are made by thermally treating nanofiber filter precursor composed of PVP at 800 °C (air) for 200 min. The resulting 3D porous filter consisting of YSZ nanofiber was stiff in a broad range of temperature condition and had low mass density (20 mg/cm^3) (Fig. 6(b), (c)). They also exhibited 99.4% $PM_{2.5}$ capturing ability and low pressure drop (ΔP=57 Pa) at an air flow rate of 4.8 cm/s and 99.97% $PM_{2.5}$ removal efficiency

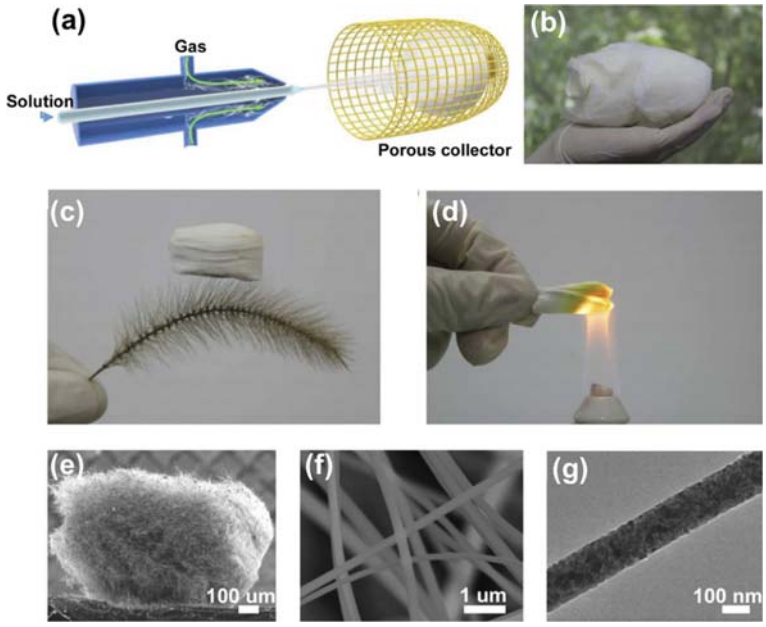

Fig. 6. (a) Schematic demonstrating the TiO_2 nanofiber filter prepared from a solution blowing process. (b) Photograph image of a Ti $(OBu)_4$/PVP sponge (c) TiO_2 filter placed on top of a green foxtail revealing the lightness of the filter. (d) Treatment with a torch indicating good heat resistance of the filter. (e) SEM image of the TiO_2 filter in (e) low magnification and in (f) high magnification. (g) TEM image of the TiO_2 nanofiber [68].

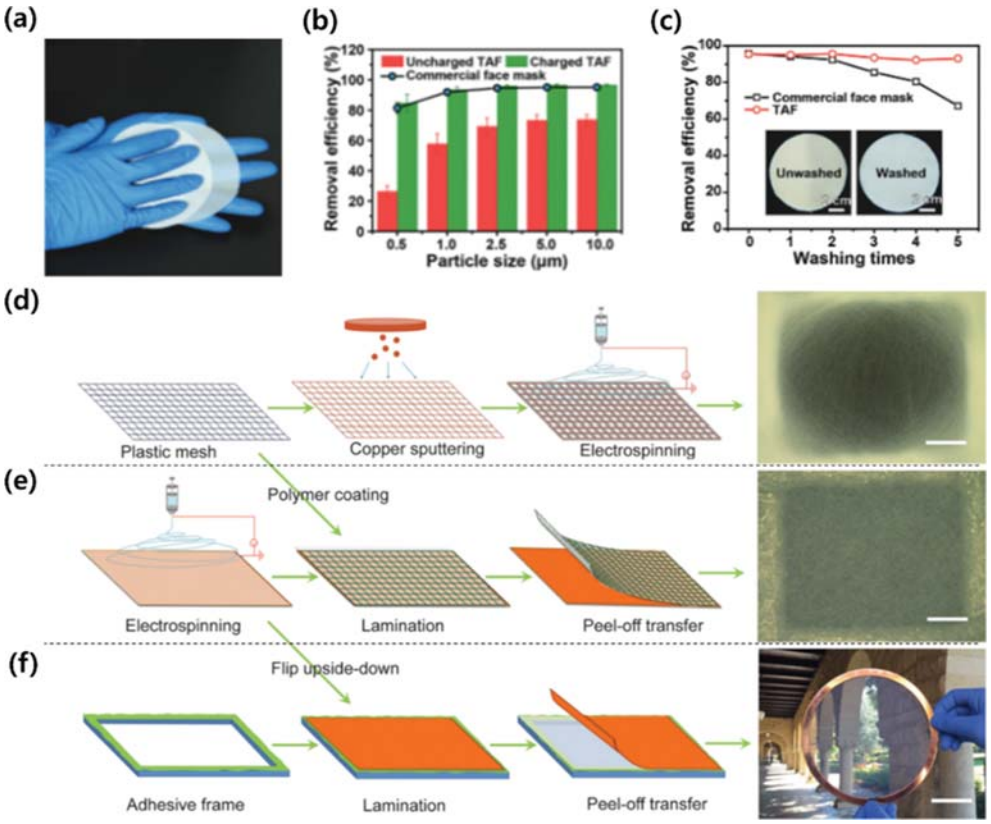

Fig. 7. (a) Photograph image showing the charging of the filter by rubbing. (b) Plot comparing the removal efficiency of the charged and uncharged state for various particle sizes. (c) Comparison between the PM removal efficiency of charged filter and commercial mask [71]. (d)-(f) Schematics and optical microscope images showing the fabrication of transparent air filter (d) by direct-spinning on a conductive mesh, and (e) by transferring electrospun nanofiber film onto a plastic mesh, and (f) by transferring of freestanding electrospun nanofiber film [74].

at 10 cm/s. Furthermore, these filters had $PM_{2.5}$ capturing ability of 98.3% even at elevated temperatures (750 °C) (Fig. 6(d)-(g)).

RECENT TRENDS IN ELECTROSPUN NANOFIBER TECHNOLOGY

Recent advances in electrospun nanofiber technology have enabled production of nanofiber filters with high filtration performance and multiple functionalities. Despite these encouraging achievements, challenges remain to be resolved to realize the broader applicability of these electrospun nanofibers for air filtration applications. These challenges include reusability and the mass production of electrospun nanofiber filters, which are currently under active investigation by many researchers [69-71]. For instance, Bai et al., developed a reusable multilayer triboelectric air filter (TAF) by using polytetrafluoroethylene (PTFE) and nylon fibers [72]. Compared to conventional electrostatic dust collectors that remove fine dust through high voltage power supply, TAF can be easily recharged by wiping the filters (Fig. 7(a)). Upon charging, TAF exhibits removal efficiency of higher than 96% for $PM_{2.5}$ and 84.7% for $PM_{0.5}$ (Fig. 7(b)). Notably, the ultra-fine dust removal efficiency increases by 3.22-times for $PM_{2.5}$ and 1.39-times for $PM_{0.5}$ compared to the uncharged state. Moreover, $PM_{2.5}$ removal efficiency remained similar even after five washing cycles and in a high humidity condition (Fig. 7(c)). This proves that TAF is applicable for commercial face masks as the filter is washable and are highly effective in removal of $PM_{2.5}$.

To date, various electrospinning methods have been explored for mass production of nanofiber filters [73]. Xu et al. proposed a new method to mass produce electrospun nanofiber by utilizing fast transfer from a metal foil to a mesh substrate (Fig. 7(d)-(f)) [74]. The nanofiber filter produced from this method exhibited high transparency (73%), superior ultra-fine dust removal (about 99.97%). Importantly, the characteristics of the nanofiber were similar, while the production rate was ten-times faster than the conventional electrospinning method. This clearly suggests that further development of such new methods will enable mass production of various types of electrospun nanofiber filters.

CONCLUDING REMARKS AND PERSPECTIVES

Providing a practical solution to air pollution, particularly for capturing fine inhalable particles ($PM_{2.5}$) in the air, is becoming urgent, critical, and challenging for our daily life and sustainable future. Among various strategies presented, electrospun nanofiber-based filtration system holds great promise in resolving this problem due to its excellent $PM_{2.5}$ capture ability offered by the small fiber diameter, high surface-to-volume ratio, low pressure drop, and controllable morphology, composition, and connectivity of the resulting nanofiber membranes.

In this review, we summarized the development of electrospun nanofiber filters with high filtration performance by starting from a brief description of the filtration mechanism and the basic principles of electrospinning process, to the structural and physical properties of the electrospun nanofiber filters. Specifically, we reviewed the recently explored polymeric fiber materials and additives that can enhance the filtration efficiency and provide additional functionality while maintaining their mechanical stability.

Although significant improvement has been made in the past few decades in the field of electrospinning, further development is required before these electrospun fibrous filters can be used in practical application. For example, in a real application, the mechanical durability should be given serious consideration, as small damage or splitting of the membrane can lead to dramatic failure in the filtration performance, restricting their use in air filtration applications. Thus, further efforts should be devoted to exploring new polymeric materials and additives that can enhance the mechanical properties of the nanofibers while retaining the versatility of the electrospinning technique. Moreover, further investigation on the structural design of the nanofibers may also provide a route to prepare more advanced filtration systems. For instance, the additional compartment offered by the core-shell structure fiber may allow fabrication of nanofiber filters with the core component providing high mechanical durability, while the outside component offers additional functionality such as reusability and antibacterial properties. This additional functionality can be achieved by either coaxial electrospinning of two separate polymer solutions or by chemical modification of a premade electrospun nanofiber filter including plasma treatment, surface polymerization, UV induced crosslinking/polymerization, and chemical immobilization of small molecules. Another important issue involves manufacture-associated problems such as cost, residual organic solvent, and production efficiency, which are an on-going challenge. Although these challenges still remain to be resolved, we anticipate that further advancement of this field will lead to providing a cost-effective, energy-saving solution to reduce $PM_{2.5}$ in the air by filtration.

ACKNOWLEDGEMENTS

This work was supported by Basic Science Research Program through the National Research Foundation of Korea (NRF) funded by the Ministry of Education (NRF-2018R1D1A1B07041102), and POSCO Green Science Program.

REFERENCES

1. Z. Zhou, Y. Liu, F. Duan, M. Qin, F. Wu, W. Sheng, L. Yang, J. Liu and K. He, *PLoS One*, **10**, 1 (2015).
2. R. B. Finkelman and L. Tian, *Int. Geol. Rev.*, **60**, 579 (2018).
3. T. Ahmad, J. Park, S. Keel, J. Yun, U. Lee, Y Kim and S. Lee, *Korean J. Chem. Eng.*, **35**, 1823 (2018).
4. C. Shim and J. Hong, *Energy Policy*, **88**, 278 (2016).
5. D. S. Martens, B. Cox, B. G. Janssen, D. B. P. Clemente, A. Gasparrini, C. Vanpoucke, W. Lefebvre, H. A. Roels, M. Plusquin and T. S. Nawrot, *JAMA Pediatr.*, **171**, 1160 (2017).
6. Y. Li, A. L. Juhasz, L. Q. Ma and X. Cui, *Sci. Total Environ.*, **650**, 56 (2019).
7. J. H. Leem, S. T. Kim and H. C. Kim, *Ann. Occup. Environ. Med.*, **27**, 7 (2015).
8. S. A. Weber, T. Z. Insaf, E. S. Hall, T. O. Talbot, A. K. Huff, *Environ. Res.*, **151**, 399 (2016).
9. A. Jaworek, A. Marchewicz, A. T. Sobczyk and A. Krupa, *T. Czech,*

Prog. Energy Combust. Sci., **67**, 206 (2018).
10. M. Babaie, P. Davari, F. Zare, M. M. Rahman, H. Rahimzadeh, Z. Ristovski and R. Brown, *IEEE Trans. Plasma Sci.*, **41**, 2349 (2013).
11. M. Tański, A. Berendt and J. Mizeraczyk, *J. Clean. Prod.*, **226**, 74 (2019).
12. Y. Yang, S. Qiao, R Jin, J. Zhou and X Quan, *Korean J. Chem. Eng.*, **35**, 964 (2018).
13. M. Park, S. Lee, J. Kim, B. Lee, J. Lee and Y. Ahn, *Part. Sci. Technol.*, **34**, 359 (2016).
14. E. M. Kettleson, J. M. Schriewer, R. M. L. Buller and P. Biswas, *Appl. Environ. Microbiol.*, **79**, 1333 (2013).
15. Y. C. Ahn, S. K. Park, G. T. Kim, Y. J. Hwang, C. G. Lee, H. S. Shin and J. K. Lee, *Curr. Appl. Phys.*, **6**, 1030 (2006).
16. S. Zhang, H. Liu, F. Zuo, X. Yin, J. Yu and B. Ding, *Small*, **3**, 1603151 (2017).
17. R. Balgis, H. Murata, T. Ogi, M. Kobayashi and L. Bao, *ACS Omega*, **3**, 8271 (2018).
18. H. Souzandeh, L. Scudiero, Y. Wang and W.-H. Zhong, *ACS Sustain. Chem. Eng.*, **5**, 6209 (2017).
19. N. Hui, X. Sun, S. Niu and X. Luo, *ACS Appl. Mater. Interfaces*, **9**, 2914 (2017).
20. C. Rao, F. Gu, P. Zhao, N. Sharmin, H. Gu and J. Fu, *Sci. Rep.*, **7**, 10366 (2017).
21. P. Zahedi, M. Fallah-darrehchi, S. A. Nadoushan, R. Aeinehvand, L. Bagheri and M. Najafi, *Korean J. Chem. Eng.*, **34**, 2110 (2017).
22. C. Wang, S. Wu, M. Jian, J. Xie, L. Xu, X. Yang, Q. Zheng and Y. Zhang, *Nano Res.*, **9**, 2590 (2016).
23. Q. Wang, Y. Bai, J. Xie, Q. Jiang and Y. Qiu, *Powder Technol.*, **292**, 54 (2016).
24. L. Fred Fu and B. A. Dempsey, *J. Membr. Sci.*, **149**, 221 (1998).
25. B. Chakrabarti, P. M. Fine, R. Delfino and C. Sioutas, *Atmos. Environ.*, **38**, 3329 (2004).
26. K. W. Lee and B. Y. H. Liu, *Aerosol Sci. Technol.*, **1**, 147 (1982).
27. R. W. Harvey and S. P. Garabedlan, *Environ. Sci. Technol.*, **25**, 178 (1991).
28. C. Yang, *Chinese J. Chem. Eng.*, **20**, 1 (2012).
29. C. Zhu, C. H. Lin and C. S. Cheung, *Powder Technol.*, **112**, 149 (2000).
30. T. Li, S. Kheifets, D. Medellin and M. G. Raizen, *Science*, **328**, 1673 (2010).
31. K. M. Steel and W. J. Koros, *Carbon*, **41**, 253 (2003).
32. R. A. Yapaulo, E. Wirojsakunchai, T. Orita, D. E. Foster, M. Akard, L. R. Walker and M. J. Lance, *Int. J. Engine Res.*, **10**, 287 (2009).
33. R. Zhang, C. Liu, P.-C. Hsu, C. Zhang, N. Liu, J. Zhang, H. R. Lee, Y. Lu, Y. Qiu, S. Chu and Y. Cui, *Nano Lett.*, **16**, 3642 (2016).
34. Y. Liao, C. H. Loh, M. Tian, R. Wang and A. G. Fane, *Prog. Polym. Sci.*, **77**, 69 (2018).
35. G. Hoek, R. M. Krishnan, R. Beelen, A. Peters, B. Ostro, B. Brunekreef and J. D. Kaufman, *Environ. Heal.*, **12**, 43 (2013).
36. K. A. Miller, D. S. Siscovick, L. Sheppard, K. Shepherd, J. H. Sullivan, G. L. Anderson, J. D. Kaufman, *N. Engl. J. Med.*, **356**, 447 (2007).
37. J. Holopainen, T. Penttinen, E. Santala and M. Ritala, *Nanotechnology*, **26**, 025301 (2015).
38. V.Aravindan, J. Sundaramurthy, P. S. Kumar, Y. S. Lee, S. Ramakrishna and S. Madhavi, *Chem. Commun.*, **51**, 2225 (2015).
39. F. Elahi, W. Lu, G. Guoping and F. Khan, *J. Bioengineer & Biomedical Sci.*, **3**, 1000121 (2013).
40. C. J. Thompson, G. G. Chase, A. L. Yarin and D. H. Reneker, *Polymer*, **48**, 6913 (2007).
41. A. Das, T. M. Schutzius, I. S. Bayer and C. M. Megaridis, *Carbon*, **50**, 1346 (2012).
42. A. K. Aljehani, M. A. Hussaini, M. A. Hussain, N. S. Alothmany and R. W. Aldhaheri, *Middle East Conf. Biomed. Eng.*, **2**, 381 (2014).
43. J.-H. Song, H.-E. Kim and H.-W. Kim, *J. Mater. Sci. Mater. Med.*, **19**, 95 (2008).
44. M. W. Lee, S. An, S. S. Latthe, C. Lee, S. Hong and S. S. Yoon, *ACS Appl. Mater. Interfaces*, **5**, 10597 (2013).
45. X. Wang and B. S. Hsiao, *Curr. Opin. Chem. Eng.*, **12**, 62 (2016).
46. S. Jiang, Y. Chen, G. Duan, C. Mei, A. Greiner and S. Agarwal, *Polym. Chem.*, **9**, 268 (2018).
47. K. A. Rieger, N. P. Birch and J. D. Schiffman, *J. Mater. Chem. B*, **1**, 4531 (2013).
48. B. Zhang, Z.-G. Zhang, X. Yan, X.-X. Wang, H. Zhao, J. Guo, J.-Y. Feng and Y.-Z. Long, *Nanoscale*, **9**, 4154 (2017).
49. T. Xia, Y. Bian, L. Zhang and C. Chen, *Energy Build.*, **158**, 987 (2018).
50. A. Patanaik, V. Jacobs and R. D. Anandjiwala, *J. Membr. Sci.*, **352**, 136 (2010).
51. R. Wakeman, *Sep. Purif. Technol.*, **58**, 234 (2007).
52. Z. Wang, C. Crandall, R. Sahadevan, T. J. Menkhaus and H. Fong, *Polymer*, **114**, 64 (2017).
53. H. J. Kim, S. J. Park, C. S. Park, T. H. Le, S. Hun Lee, T. H. Ha, H. I. Kim, J. Kim, C. S. Lee, H. Yoon and O. S. Kwon, *Chem. Eng. J.*, **339**, 204 (2018).
54. A. Zucchelli, M. L. Focarete, C. Gualandi and S. Ramakrishna, *Polym. Adv. Technol.*, **22**, 339 (2011).
55. S. Zhang, N. A. Rind, N. Tang, H. Liu, X. Yin, J. Yu and B. Ding, *Electrospun Nanofibers for Air Filtration*, in: B. Ding, X. Wang, J Yu. Electrospinning: Nanofabrication and Applications, Elsevier, 365 (2019).
56. S. K. Nataraj, K. S. Yang and T. M. Aminabhavi, *Prog. Polym. Sci.*, **37**, 487 (2012).
57. D. Cho, A. Naydich, M. W. Frey and Y. L. Joo, *Polymer*, **54**, 2364 (2013).
58. Q. Zhang, J. Welch, H. Park, C.-Y. Wu, W. Sigmund and J. C. M. Marijnissen, *J. Aerosol Sci.*, **41**, 230 (2010).
59. F. Mokhtari, M. Salehi, F. Zamani, F. Hajiani, F. Zeighami and M. Latifi, *Text. Prog.*, **48**, 119 (2016).
60. K. Liu, C. Liu, P.-C. Hsu, J. Xu, B. Kong, T. Wu, R. Zhang, G. Zhou, W. Huang, J. Sun and Y. Cui, *ACS Cent. Sci.*, **4**, 894 (2018).
61. A. Khang, P. Ravishankar, A. Krishnaswamy, P. K. Anderson, S. G. Cone, Z. Liu, X. Qian and K. Balachandran, *J. Biomed. Mater. Res. - Part B Appl. Biomater.*, **105**, 2455 (2017).
62. X. Huang, T. Jiao, Q. Liu, L. Zhang, J. Zhou, B. Li and Q. Peng, *Sci. China Mater.*, **62**, 423 (2019).
63. K. Watanabe, B.-S. Kim and I.-S. Kim, *Polym. Rev.*, **51**, 288 (2011).
64. S. Zhang, H. Liu, X. Yin, J. Yu and B. Ding, *ACS Appl. Mater. Interfaces*, **8**, 8086 (2016).
65. O. Yildiz, K. Stano, S. Faraji, C. Stone, C. Willis, X. Zhang, J. S. Jur and P. D. Bradford, *Nanoscale*, **7**, 16744 (2015).
66. M. Nogi, S. Iwamoto, A. N. Nakagaito and H. Yano, *Adv. Mater.*,

21, 1595 (2009).
67. C. Liu, P.-C. Hsu, H.-W. Lee, M. Ye, G. Zheng, N. Liu, W. Li and Y. Cui, *Nat. Commun.*, **6**, 6205 (2015).
68. H. Wang, X. Zhang, N. Wang, Y. Li, X. Feng, Y. Huang, C. Zhao, Z. Liu, M. Fang, G. Ou, H. Gao, X. Li and H. Wu, *Sci. Adv.*, **3**, e1603170 (2017).
69. S. Jeong, H. Cho, S. Han, P. Won, H. Lee, S. Hong, J. Yeo, J. Kwon and S. H. Ko, *Nano Lett.*, **17**, 4339 (2017).
70. X. Zhao, Y. Li, T. Hua, P. Jiang, X. Yin, J. Yu and B. Ding, *Small*, **13**, 1603306 (2017).
71. Y. Bai, C. B. Han, C. He, G. Q. Gu, J. H. Nie, J. J. Shao, T. X. Xiao, C. R. Deng and Z. L. Wang, *Adv. Funct. Mater.*, **28**, 1706680 (2018).
72. B. Khalid, X. Bai, H. Wei, Y. Huang, H. Wu and Y. Cui, *Nano Lett.*, **17**, 1140 (2017).
73. Y. Chen, S. Zhang, S. Cao, S. Li, F. Chen, S. Yuan, C. Xu, J. Zhou, X. Feng, X. Ma and B. Wang, *Adv. Mater.*, **29**, 1606221 (2017).
74. J. Xu, C. Liu, P.-C. Hsu, K. Liu, R. Zhang, Y. Liu and Y. Cui, *Nano Lett.*, **16**, 1270 (2016).

Biography: Hyomin Lee received his B.S. in Chemical and Biological Engineering from Seoul National University (SNU) in 2009. He obtained Ph.D. degree in Chemical Engineering from Massachusetts Institute of Technology (MIT) in 2014. From 2014 to 2017, he worked as a postdoctoral researcher in John A. Paulson School of Engineering and Applied Sciences at Harvard University. In 2017, he joined Pohang University of Science and Technology (POSTECH), where he is currently an assistant professor in the department of chemical engineering. He has been recognized with several awards including AIChE Graduate Student Award (2014), KSIEC New Scientist Award (2018). His research focuses on understanding and controlling the structure and dynamics of soft matter at interfaces and designing new functional materials.